CLIMATE PATTERN RECOGNITION OVER 3000 YEARS OF THE HOLOCENE ONSET (8500 BC TO 5500 BC)

JOACHIM SEIFERT

FRANK LEMKE

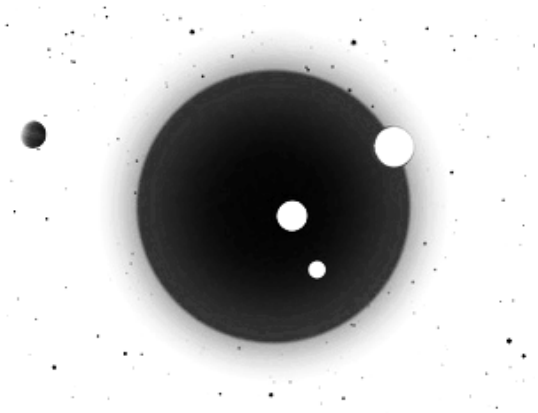

Correspondence to: weltklima@googlemail.com

Website: http://www.knowledgeminer.eu • http://www.climateprediction.eu

DECEMBER 2014

Abstract. Features and application of the Climate Pattern Recognition method for evaluating temperature evolution in Holocene time series are explained. We select as the first period, the early 3000 years of the Holocene. This study recognizes four distinct climate patterns, the multi-millennial pattern, two multi-centennial patterns and one short multi-decadal pattern. Special attention is given to peak temperature spikes. The analysis is able to distinguish different causes of climate change out from Holocene temperature graphs, such as the Milankovitch line, Earth orbit oscillations, cosmic meteor impacts on Earth and likely volcano mega-eruptions. We use the graphical version of GISP2 for visual demonstration of climate patterns. Each up and down of the GISP2 temperature curve is explained in detail. We were able to identify the causes for cyclic Bond events and causes for other cyclic temperature oscillations in the Holocene. A well-defined continuous multi-centennial Holocene cycle with 7-year growing periods is proven for the entire Holocene. Its exact timing of the cycle excludes an internal atmospheric-oceanic cycle cause. The pattern recognition method determines the indisputable celestial origin of cyclic patterns and is superior to GCM/PMIP/CMIP models, which all underperformed in recent 2014 model-data comparisons. We divide the Holocene into 5 intervals and continue for the time span BC 7000 to BC 4300 in the second paper.

Citations. Seifert, J., Lemke, F.: Climate Pattern Recognition over 3000 Years of the Holocene Onset (8500 BC to 5500 BC), 2014,
http://www.knowledgeminer.eu/climate_papers.html

1. INTRODUCTION

In the last decade, GCM climate models of type PMIP2/3 and CMIP3/5 were vaunted as major millennial climate science achievement. The accuracy of models was characterized with certainty classification levels of very likely, extremely likely and virtually certain, with 99.9% of statistical probability.

Over the past 2 years, however, those models were tested in independent model-data comparisons showing underperformance in all climate aspects, e.g. in temperature evolution (McKitrick, 2014), in global atmospheric circulation and precipitation in the Holocene (Alder and Hostetler, 2014), in modeling the last interglacial (Bakker and Reussen, 2014), and in aeolian dust of 23 CMIP5 models (Evan, 2014). Holocene models were especially wanting; large periods remain in enigma or "conundrum" (Liu, 2014). Reasons for low model performance are known: A deterministic parameterization, use of tuned coefficients and built-in fudge factors (Pielke Sr., 2013) as a result of insufficient a priori knowledge of the internal workings of the climate system, which is characteristic for complex systems in general (Lemke, 2011). A logical development now is that alternative climate studies without GCMs increasingly appear. Examples are the harmonic solar and planetary approach of N. Scafetta (Scafetta, 2013), or the stochastic, non-Markovian approach of Franzke (Franzke, 2014), or a "Simple Harmonic Model" of (Solheim and Humlum, 2013), or an "Optimal Ranking Regime" approach of (Mauget, 2014) and a variety of others. However, all

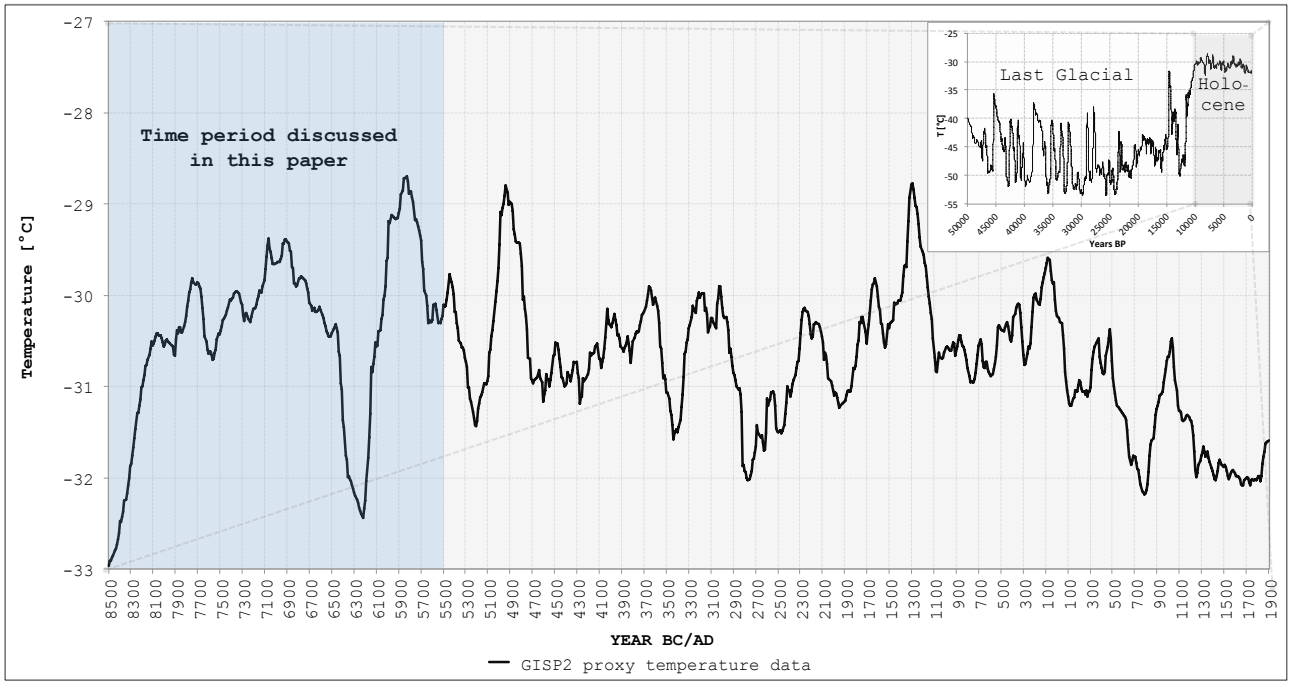

Figure 1. The Holocene GISP2 data and the period discussed in this paper (equidistant in time)

alternative approaches need verification on long millennial time frames.

In this paper, we present major features of the Climate Pattern Recognition Analysis, showing four, mostly cosmic-driven major patterns of climate forcing over a multi-millennial time frame.

For this pattern recognition, we need a high resolution time series in a graphical form, from which all patterns can be identified. The GISP2 ice-core temperature series (Alley, 2000) is an excellent reference, which we transformed into an equidistant time series with a resolution of 10 years to allow easy display of periodic processes. The resulting Holocene GISP2 graph and the time period discussed in this paper is shown in figure 1.

Our analysis will reveal four visible patterns, which we present from the longest-term to the shortest-term pattern.

2. THE LONG-TERM MULTI-MILLENNIAL PATTERN

Milankovitch cycles are universally known, and they range in time between 21,400 and 100,000 years and need not to be discussed in this paper. They produce very slowly increasing/decreasing average temperatures on

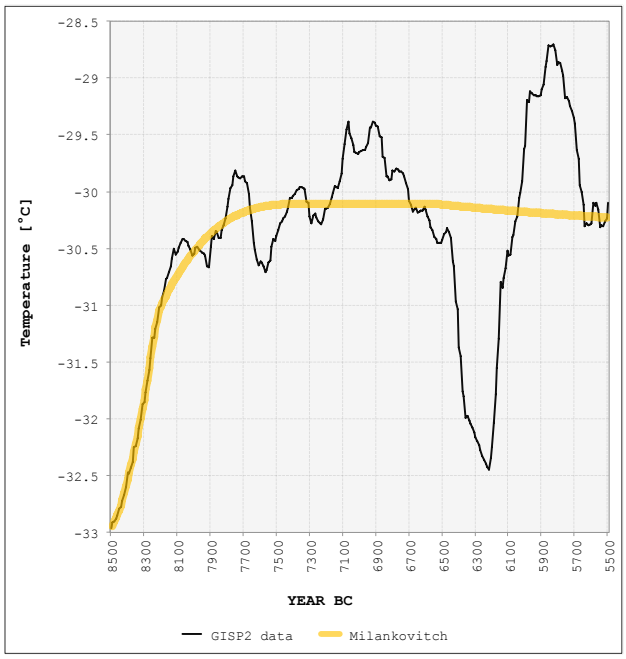

Figure 2. Masson-Demotte-Milankovitch Line and GISP2

Earth, and are not responsible for abrupt climate changes on multi-centennial scale. We utilize the curvilinear Milankovitch pattern line, as first step of pattern recognition. The line is given in (Masson-Delmotte, 2005) and we insert this Masson-Delmotte-Milankovitch line directly into the GISP2 temperature curve (fig. 2).

In this graph, we can recognize the continuous and rather strong upward temperature evolution from the glacial period into the Holocene. While the rising curvilinear Milankovitch line slowly and smoothly reaches the temperature top, a new pattern develops: Oscillation around the Milankovitch line commences and increases in amplitude and period. This oscillation around the Milankovitch line is the second climate pattern.

3. THE REGULAR MULTI-CENTENNIAL PATTERN OF THE EARTH ORBIT OSCILLATION

Since 1997, multi-centennial Holocene patterns or oscillations are known as “Bond cycles or events”. Their causes are unknown and the Bond cycle pacing is kept vague at 1470 ±500 years. No proper cycle beginnings and endings were given by Bond, and cycle length fluctuations may vary between 970 and 1970 years. Additionally, there exist only one single clear event signal (for the 8.2 kyear cooling event) for 8 cycles. This huge uncertainty, of cause, gives room for speculation on the “Bond cycle” cause: The present discussion is polarized between internal forcing through ocean circulation vs. external solar forcing. We will take a look at the ultimate available paper on the subject, as of December 2014, (Evangelista, 2014). The paper employs the Morlet-wavelet analysis for the time period 11,100 BC to 2,100 BC, and detects “marked periodic signals of ~0.8, ~1.7 and ~2.2 kyears," thus, a marked around 800 year cycle. According to Soon (Soon, 2014) “the 1500-1800 year periodicity is widely represented in paleoclimatic records,” but as being twice an ~800 year span, “... may represent the same or two separate cycles”. The major Holocene cycle, obviously, is the ~800 year cycle, and other 1500-1800 year cycles are derived multiples with vague pacing. The Evangelista paper shows the ~800-year empirical evidence for the 790-year “Klimawelle” cycle (Earth Orbit Oscillation, EOO), as calculated by Seifert in 2010 (Seifert, 2010). More Holocene cycle literature (Seifert and Lemke, 2012) graphically shows that the Holocene also contains smaller oscillations in its early phase, increasing slowly towards the present Current Warm Period (CWP). For this reason Soon (Soon, 2014) identified “intermediary derived cycles at 700-yr and 300-yrs”.

The 1470-year cycle is Bond´s copied number of 1470-year D-O-events, visibly between 27ka and 37ka BP. The origin and true causes of D-O events between 27 and 37 ka BP are covered in detail in (Seifert and Lemke, 2012). The 790-year cycle study (Seifert, 2010) explains cycle calculation procedures and proves a linear relation between cycle oscillation amplitude and oscillation period.

We will examine whether a steadily growing, well defined periodicity exists within the Holocene. The error should not exceed 1 decade and the periodicity must be detectable for 10,000 years. Finding such a well-defined periodicity would prove an indisputable external celestial cyclic forcing, because, as Stocker showed in 1992 (Stocker and Mysak, 1992), that the internal atmosphere-ocean climate system is unable to produce a forcing with "a single, well defined periodicity". This would permit us to substitute the internal forcing by a periodic Holocene climate driver.

We will use the Climate Pattern Recognition method in order to resolve this cyclic oscillation question and proceed to pattern observation in figure 3.

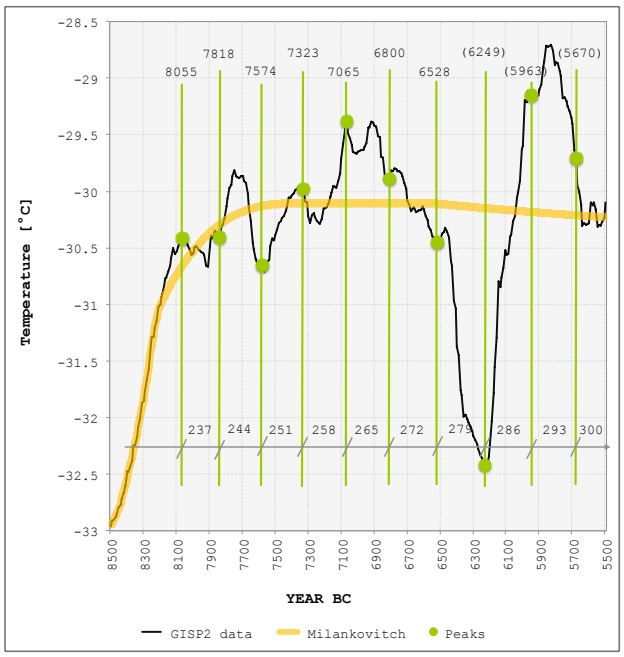

Figure 3. Milankovitch Line and Cosmic Oscillation Pacing

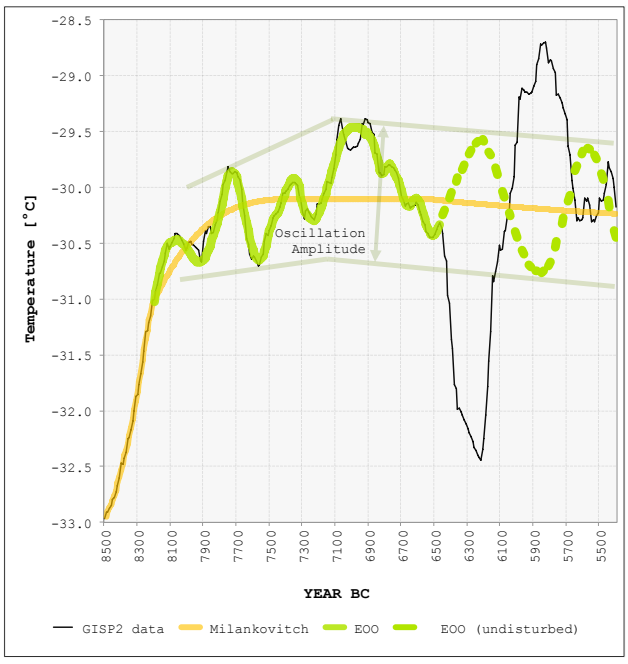

Figure 4. Formation of EOO Wave

We see the following: The yellow Milankovitch line helps us to identify the central line between oscillations either to the above or to below the line. Before analyzing temperature oscillation amplitudes, we identify the regular oscillation period in 3 steps:

Step 1: The first date for peak oscillation from the Milankovitch line is BC 8055. The following date of oscillation, now to below this line, is BC 7574, a time span of 481 years.

Step 2: We divide those 481 years into two parts, as a sine semi-wave. As the oscillation period is supposed to be growing, we set the first, shorter wave part to 237 years, and the second part, 7 years longer, to 244 years, together a sum of 481 years.

Step 3: We use the semi-wave oscillation period of 237 years as basic period and prolong it by 7 years for each following period. The starting point is 8055 BC. The prolonging period dates are 8055-7818-7574-7323-7065-6800-6528-(6249)-(5963)-(5670) BC, the latter 3 masked, the reason is the third type of patterns. These well-defined period dates continue visibly for the next 10,000 years, which will be demonstrated in additional Holocene papers.

In figure 4 we can see the following: The growing period length is regular, being dictated by celestial force, pacing a 7 year period prolongation. The pacing is obvious, but a sine-oscillation amplitude has not fully formed yet and the wave seems to try to squeeze into much too short period distances.

After temperatures reached their maximum height at 7100 BC, the sine wave finally starts regularly in BC 6500, but masked by an abrupt Z-shaped pattern. The regular sine-pattern will appear after the end of the interrupting Z-pattern. At 7000 BC, the sine amplitude has a GISP2 borehole temperature difference of 1.1°C. As the Holocene progresses to the CWP, both cycle period and amplitude increase by about 70%. Reaching the CWP, the cycle amplitude is 1.8°C on the GISP2 borehole temperature scale. Finally, we compare the determined Holocene periods with calculations of period lengths, according to Seifert (Seifert, 2010) and to the graphical method of period identification, according to (Seifert and Lemke, 2012). This comparison reveals, that the 7-year oscillation prolongation is about 1% too long, and, therefore, needs to be reduced to a 6.95 years prolongation. This reduction will not change much the period dates in the Early Holocene, only the last dates by 1-2 years, which change to 6250, 5964, 5672, and 5372 BC. Those small period

adaptions improve significantly the tail end period signals in the MWP (AD 1208), in the LIA (AD 1640) and in the CWP (AD 2078). As final remark, the EOO Earth orbital oscillation pattern is not a Milankovitch cycle pattern, but is a different cycle as described by the mathematician Carl Gauss in 1809 (Gauss, 1809).

The reason for this prolonging pacing of 6.95 years is also clear, as explained in (Seifert, 2010): The EOO orbital oscillation is a linear function of the apsidal precession of the Earth orbital plane. Therefore, as Earth exits the glacial time (with the Milankovitch line), the apsidal precession receives a maximum boost and commences with a maximum value, which produces the shortest EOO period of 481 years. In the course of millennia, this precessional boost effect subsides, the apsidal precession gets less (the 21,600 year time frame shortens continuously) and the EOO semi-waves prolong by a steady pacing of 6.95 years, which is visible in the GISP2 record.

4. THE ABRUPT, STOCHASTIC, Z-SHAPED MULTI-CENTENNIAL PATTERN

At 6528 BC, the oscillatory bottom point of the temperature line was reached and temperatures turns around upwards to rise for 80 years. But at 6450 BC, a powerful interruption of the oscillation pattern occurred, the "8.2 kiloyear event". This event marks our third recognizable pattern: It is a centennial, interrupting Z-shaped stochastic pattern, which overrides, cancels out and masks the visible green EOO oscillation line.

Both patterns, the oscillatory cyclic pattern and this strong stochastic disturbance pattern, are entirely separate processes. This overriding, masking pattern is more forceful than the oscillatory wave line, which simultaneously, but invisibly, continues as well. The oscillatory wave is visible again at the end of the Z-pattern, at BC 5600.

A dominant feature of the interrupting Z-pattern are pronounced top and bottom spikes. The Z-pattern commences at 6450 BC. The abrupt event sent the global temperature in a steep line downwards to its bottom spike at 6220 BC. From there, an abrupt turnaround sets in and the temperature rebounds straight to the next top temperature spike, much higher than the 6450 BC interruption date. We place a horizontal level line into the Z-pattern, in order to show the pattern´s beginning and end. The cause of this wide swing Z-shaped temperature oscillation is the impact of a cosmic meteor on Earth. The mechanics of this process is outlined in (Seifert and Lemke, 2012), pointing out a number of empirical cosmic events, all of which produce a Z-shaped GISP2 temperature pattern. Additionally, the Z-temperature swing relates to the size of impact craters, therefore, small meteor impacts produce small Z-shaped temperature swings and large impacts produce large temperature swings.

The cosmic meteor impact at 6450 BC is known as the "Storegga slide". The meteor bolide hit the headwall of the Norwegian continental shelf, coming from the East, to the West, with the crater located 200 m below ocean level, which pushed an enormous rock volume from the steep continental edge over hundreds of kilometers along the ocean floor. All Storegga literature, at present, hypothesize the slide as being an earthquake slide and doubt this at the same time, because the huge slide volume is too much to be a sole earthquake effect. The displaced rock mass is estimated at an enormous 2,500-3,200 km^3 volume. Two large historical volcano mega-eruptions, as comparison, ejected 10 km^3 mass volume (the Pinatubo eruption, 1991) or 60 km^3 mass volume (the giant Thera-Santorini eruption, 1603 BC). Methane pressures in sediments are hypothesized as additional triggering force, but the so-called "suspected gas hydrate-pressure" is relieved in the whole area by multitudes of "pockmarks", which are large vertical gas pressure relieve vents, for discharge of underground gases. The Storegga slide is indisputably caused by a cosmic meteor impact. The impact crater lies at the coordinates of 64°N and 5°E. The crater is well visible on perspective seafloor bathymetrical maps. Comprehensive evidence will be given in a separate Storegga cosmic impact paper in 2015. Sea floor mapping identified a total of four craters (Solheim and Bryn, 2005).

Another 2015 paper will deal with solar system and meteor impact mechanics on Earth.

The comet impact pattern lasts from 6450 BC to 5600 BC. After the end of this masking Z-pattern, the GISP2 temperature line moves upwards to bridge the gap to the green EOO down-moving oscillation line. As both lines unite in 5450 BC, temperatures fall and follow the cyclic EOO pattern for the next decades.

5. THE STOCHASTIC MULTI-DECADAL PATTERN (VOLCANO MEGA-ERUPTION)

Figure 5 shows two occasions of a multi-decadal temperature dip and recovery. We assume that those V-shaped temperature dips are climatic effects of VEI 6, 7 and 8 mega-eruptions of stratospheric volcanos, causing stratospheric dimming for decades, and temporary cooling. Only a small minority of volcanos can achieve a persistent stratospheric effect over decades. Calculations for regular, short eruption effects are made in (Wahl, 2014), showing "a clear and robust 3 - 5 years La Nina-like response". The two blue V-shaped temperature dips in figure 5 might indicate possible volcano mega-eruptions,

at 7100 BC and 5550 BC, but this presumption needs further study. A stratospheric volcano candidate could be Mt. Takahe in Antarctica, 3460 m high, with a proven 5550 BC mega-eruption.

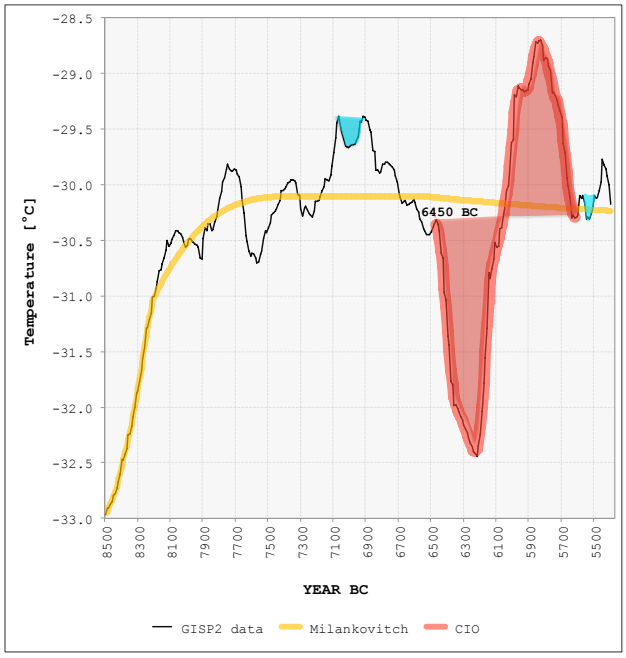

Figure 5. Milankovitch, cosmic impact, and volcano eruption dimming

6. SYNOPSIS

We combine all climate forcing patterns in one single diagram and explain the successive phases of temperature evolution in figure 6.

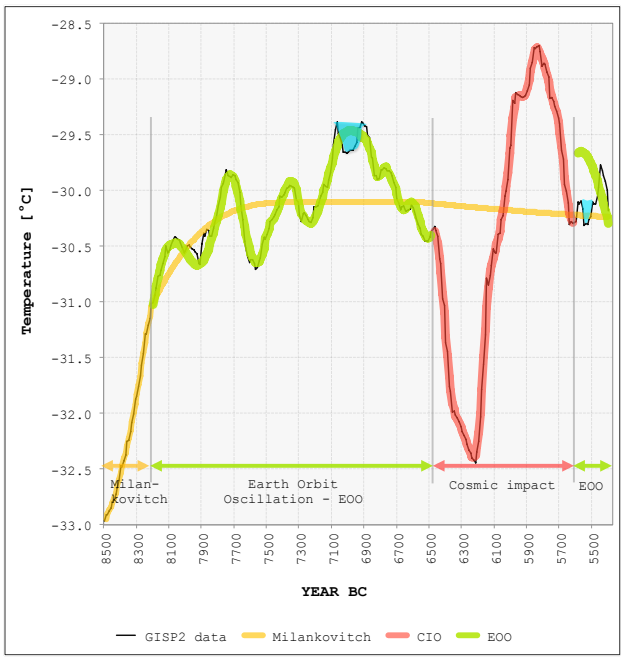

Figure 6. Temperature pattern synopsis

On the left, the yellow Milankovitch line rises out of the Last Glacial Maximum. In 8300 BC, gradually and still irregular, Earth orbit oscillations (green line) start out of this line. A celestial mechanism dictates a well-defined multi-centennial oscillation pace which prolongs by 13.9 years at each successive cycle. The cycle dates are provided. The cyclic temperature evolution becomes suddenly masked, starting 6450 BC, when a large cosmic meteor hit Earth and initiated a wide-swing Z-shaped temperature oscillation (red line). This oscillation swing stabilizes in 5600 BC, when temperatures returned to their initial level of 6450 BC. From 5600 BC on, temperatures rise again in order to join the invisible green cycle pattern line. Reaching this oscillatory line, temperatures go down according to the cyclic pattern. Furthermore, two large mega-volcano eruptions (blue areas) appear to mark short V-dips in the GISP2 temperature line. We continue the pattern analysis in additional papers for the entire Holocene. In AD-times, the Roman-WP, the Migration-CP, MWP, LIA, and the CWP are visibly on hand. The pattern analysis is suitable to identify shorter decadal cycles as well. In early 2015, the next available paper demonstrates the "origin and causes of the ~60 year Holocene cycle".

REFERENCES AND SOURCES

Alder, J.R.; Hostetler, S.W.: Global climate simulations at 3000 year intervals for the last 21000 years with the GENMOM coupled atmosphere-ocean model, Clim. Past. Discuss., 10, 2925-2978, 2014, DOI: 10.5194/cpd-10-2925-2014

Alley, R.B.: The Younger Dryas cold interval as viewed from central Greenland, Quaternary Science Reviews, Volume 19, Issues 1-5, 2000, http://www.ncdc.noaa.gov/paleo/icecore/greenland/greenland.html,

Bakker, P.; Reussen, H.: Last interglacial model-data mismatch of the thermal maximum temperatures partially explained, Clim.Past.,10, 1633-1644, 2014, DOI: 10.5194/cp-10-1633-2014

Evan, A.T., et.al.: An analysis of aeolian dust in climate models, Geophys. Res. Lett., 41, online 18.Aug. 2014, DOI: 10.1002/2014GL060545

Evangelista, H.; et.al.: South Tropical Atlantic anti-phase response to Holocene Bond Events, Palaeogeography, Palaeoclimatology, Palaeooecology, vol. 415, Dec. 2014, p. 21-27, doi: 10.1016/j.palaeo.2014.07.019

Franzke, Ch. L.E. et al: Stochastic Climate Theory and Modelling, Sept 1, 2014, arXiv:1409.0423 [physics.ao-ph]

Gauss, Carl: Theoria Motus Corporum Coelestium, Perthes&Besser publishers, Hamburg, 1809, http://dx.doi.org/10.3931/e-rara-522

Lemke, F.: What Drives Global Warming?, Global Warming Prediction Project, 2011, http://is.gd/xnczGE

Liu, Z. et. al.: The Holocene Temperature Conundrum, PNAS, vol. 111, no. 34 (2014) DOI: 10.1073/pnas.1407229111

Masson-Delmotte, V. et al : GRIP Deuderium Excess Reveals Rapid and Orbital-Scale Changes in Greenland Moisture Origin, Science, vol 309 (2005), no.5731, pp. 118-121, displayed in figure 1, at right: Obliquity fluctuations

Mauget, S.A.; Cordero, E.C.: Optimal Ranking Regime Analysis of Intra- to Multi-Decadal U.S. Climate Variability, AMS, Journal of Climate, e-view, 2014, DOI: http://dx.doi.org/10.1175/JCLI-D-14-00040.1

McKitrick, R.R.: HAC-robust Measurement of the Duration of a Trendless Subsample in a Global Climate Time Series. Open Journal of Statistics, 4, 2014, pp527-535, http://dx.doi.org/10.4236/ojs.2014.47050

Pielke, Sr., R.A.: Mesoscale meteorological modelling, 3rd. edition, Academic Press, 2013, 760 p., ISBN 9780123852373, chapter 7 and 8

Scafetta, N.: Solar and Planetary Oscillation Control on Climate Change: Hindcast, Forecast and a Comparison with the CMIP5 GCMs, Journal Energy and Environment, vol. 24, no. 3-4, June 2013, pp. 455-496, DOI: 10.1260/0958-305X.24.3-4.455

Seifert, J.: Das Ende der globalen Erwärmung, Berechnung des Klimawandels, ISBN 978-3-86805-604-4, Pro Business Verlag, 2010, 109 pages, pp.53-56 www.book-on-demand.de

Seifert, J., Lemke, F.: Five climate forcing mechanisms govern 20,000 years of climate change, 2012, http://www.knowledgeminer.eu/climate_papers.html

Solheim, A., Bryn, P: Ormen Lange - An integrated study for the safe field development in the Storegga slide area, Elsevier, 2005, ISBN 0080446949, p.1-10, reprint from Marine and Petroleum Geology, vol. 22/1-2, 2005

Solheim, J.-E., Humlum, O.: "En enkel empirisk harmonisk klimamodell", in: Geoforskning, No 5, August 2013

Soon, W.; et.al.: A review of Holocene solar-linked climatic variation on centennial to millennial time scales: Physical processes, interpretative frameworks and a new multiple cross-wavelet transform algorithm, Earth-Science Reviews, vol. 134, Jul 2014, p.1-15, doi: 10.1016/j.earscirev.2014.03.003

Stocker, T.F., Mysak, L.A.: Climatic fluctuations of the century time scale: A review of high-resolution proxy data and possible mechanisms, Climate Change, 20, p. 227-250, March 1992, Kluver Academic Publishers, N.L., http://www.climate.unibe.ch/~stocker/papers/stocker92cc.pdf

Wahl, E.R., et.al: Late winter temperature response to large tropical eruptions in temperate western Northern America: relationship to ENSO phases, Global and Planetary Change, vol. 122, 2014, pp. 238 - 250, DOI: 10.1016/j.gloplache.2014.08.005